Bisphenol A facilitates bypass of androgen ablation therapy in prostate cancer

Yelena B. Wetherill,[1] Janet K. Hess-Wilson,[1] Clay E.S. Comstock,[1] Supriya A. Shah,[1] C. Ralph Buncher,[2] Larry Sallans,[3] Patrick A. Limbach,[3] Sandy Schwemberger,[4] George F. Babcock,[4] and Karen E. Knudsen[1,5,6]

[1]Department of Cell and Cancer Biology, [2]Department of Environmental Health, [3]Rieveschl Laboratories for Mass Spectrometry, Department of Chemistry, [4]Department of Surgery/Shriners Hospital for Children, [5]Center for Environmental Genetics, and [6]University of Cincinnati Cancer Center, University of Cincinnati College of Medicine, Cincinnati, Ohio

Abstract

Prostatic adenocarcinomas depend on androgen for growth and survival. First line treatment of disseminated disease exploits this dependence by specifically targeting androgen receptor function. Clinical evidence has shown that androgen receptor is reactivated in recurrent tumors despite the continuance of androgen deprivation therapy. Several factors have been shown to restore androgen receptor activity under these conditions, including somatic mutation of the androgen receptor ligand-binding domain. We have shown previously that select tumor-derived mutants of the androgen receptor are receptive to activation by bisphenol A (BPA), an endocrine-disrupting compound that is leached from polycarbonate plastics and epoxy resins into the human food supply. Moreover, we have shown that BPA can promote cell cycle progression in cultured prostate cancer cells under conditions of androgen deprivation. Here, we challenged the effect of BPA on the therapeutic response in a xenograft model system of prostate cancer containing the endogenous BPA-responsive AR-*T877A* mutant protein. We show that after androgen deprivation, BPA enhanced both cellular proliferation rates and tumor growth. These effects were mediated, at least in part, through androgen receptor activity, as prostate-specific antigen levels rose with accelerated kinetics in BPA-exposed animals. Thus, at levels relevant to human exposure, BPA can modulate tumor cell growth and advance biochemical recurrence in tumors expressing the AR-*T877A* mutation. [Mol Cancer Ther 2006;5(12):3181–90]

Introduction

Prostate cancer is the second leading cause of cancer death among males in the United States and the most commonly diagnosed malignancy (1). Organ-confined prostate cancer is associated with favorable outcome, as local disease can be effectively treated through radical prostatectomy or radiation therapies (reviewed in refs. 2–5). However, disseminated disease is treated based on the androgen dependence of the tumor, and androgen deprivation therapy (ADT) is the first line of therapeutic intervention (6, 7). Although ADT is initially effective, within 18 to 30 months recurrent tumors ultimately arise, for which no effective treatment has been identified (8–10). As such, there is an urgent need to identify factors that influence the imminent transition to therapy resistance.

ADT centers on ablation of androgen receptor function, an androgen-dependent transcription factor whose activities are required for prostate cancer growth and progression (11). In ADT, androgen receptor function is blocked either through inhibition of androgen synthesis as achieved through chemical or surgical means (6) and/or through the use of androgen receptor antagonists that inhibit androgen receptor activity via direct interaction (12–15). ADT strategies are typically successful, as monitored by both tumor regression and a reduction in *prostate-specific antigen* (*PSA*) expression, a known androgen receptor target gene used clinically to monitor prostate cancer progression (16). A plethora of evidence shows that androgen receptor activity is inappropriately restored in recurrent tumors leading to therapeutic resistance. The androgen receptor is aberrantly activated in late-stage prostate cancer through multiple mechanisms, including androgen receptor amplification, ligand-independent androgen receptor activation, or gain-of-function androgen receptor mutations (17–22). Several tumor-derived androgen receptor mutations are known to change the conformation of the ligand-binding domain and allow activation of the receptor by non-canonical ligands. For example, the AR-*T877A* mutant results in the ability of the receptor to use androgen, estrogen, progestins, and anti-androgens as ligands (23–26). This specific mutation is reported to occur in up to 31% of advanced prostate tumors (27) and is present in the LNCaP model system of prostate cancer.

Received 5/11/06; revised 9/5/06; accepted 10/13/06.

Grant support: NIH grant RO1-CA 093404 (K.E. Knudsen), NIH grant RR019900 (to P.A. Limbach), National Institute of Environmental Health Sciences Center for Environmental Genetics core grant E30-ES-06096, and National Institute of Environmental Health Sciences Environmental Mutagenesis and Cancer training grant ES-07250-16 (Y.B. Wetherill and J.K. Hess-Wilson).

The costs of publication of this article were defrayed in part by the payment of page charges. This article must therefore be hereby marked advertisement in accordance with 18 U.S.C. Section 1734 solely to indicate this fact.

Note: Y.B. Wetherill and J.K. Hess-Wilson contributed equally to this work.

Requests for reprints: Karen E. Knudsen, Department of Cell and Cancer Biology, Vontz Center for Molecular Studies, University of Cincinnati College of Medicine, 3125 Eden Avenue, ML 0521, Cincinnati, OH 45267-0521. Phone: 513-558-7371; Fax: 513-558-4454. E-mail: Karen.Knudsen@uc.edu

doi:10.1158/1535-7163.MCT-06-0272

We showed previously that a subset of prostate cancer cell lines harboring androgen receptor mutations might be susceptible to growth stimulation by the known endocrine-disrupting compound bisphenol A (BPA; refs. 28, 29). BPA is used in the manufacture of polycarbonate plastics and epoxy resins and is leached from these materials into food and water supplies (30). A recent study shows that 95% of adults in the United States have detectable BPA in their urine (31). In previous studies, we showed that select androgen receptor tumor-derived mutants can be activated by BPA, and BPA can cooperate with low-level androgen to enhance mutant androgen receptor activity (29). Moreover, we showed that this action of BPA stimulated cell cycle progression in LNCaP cells under conditions of androgen deprivation (28). Although these studies suggested that exposure to endocrine-disrupting compounds may influence the cellular response to ADT, the effect on therapeutic response *in vivo* had yet to be assessed. Here, we challenged the consequence of BPA on ADT *in vivo* using a well-established xenograft model of prostate cancer. Our data indicate that after androgen ablation, environmentally relevant levels of BPA stimulated tumor cell proliferation and enhanced tumor growth. In addition, animals exposed to BPA exhibited a shorter time to therapeutic resistance, shown by a more rapid increase in PSA. Together, these data show that incidental environmental exposure to BPA may advance the transition to therapeutic resistance in a subset of prostate cancers harboring BPA-responsive mutations of the androgen receptor.

Materials and Methods

Animals

NCR/*nu/nu* (athymic) male mice, 6 to 8 weeks of age, were purchased from the Animal Production Area of the National Cancer Institute-Frederick Cancer Research Facility (Frederick, MD). The mice were housed in cages fitted with a high efficiency filter top in animal facilities approved by the American Association for Accreditation of Laboratory Animal Care. The room was kept at 25°C with a 12-h light-dark cycle. All of the animal studies were conducted in accordance with the principles and procedures outlined by the NIH guidelines and the Institutional Animal Care and Use Committee of the University of Cincinnati (Cincinnati, OH).

Assessment of Tumor Growth *In vivo*

LNCaP cells between passages 32 to 37 were cultured in improved MEM (Biofluids, Rockville, MD) supplemented with 5% fetal bovine serum (HyClone, Logan, UT), 100 units/mL penicillin/streptomycin, and 2 mmol/L L-glutamine (Mediatech, Herndon, VA). Cells were grown at 37°C in a 5% CO_2 humidified incubator. Before inoculation, LNCaP cells were washed, trypsinized, and resuspended in phenol red–free improved MEM supplemented with 5% charcoal dextran–treated (CDT) serum. LNCaP cells were then combined with Matrigel (Becton Dickinson, Bedford, MA) at 3:1 volume ratio of medium to Matrigel, and a total of 2×10^6 cells in 100 μL was inoculated s.c. in the right flanks of 6- to 8-week-old male nude mice. Mice were housed and monitored for tumor growth every week. Most tumors were established 6 to 8 weeks postinjection with a tumor take of ~60%, consistent with what has been reported in the literature (32). Tumor volumes were measured using a caliper and expressed in mm^3 using the following formula: volume (mm^3) = long diameter (mm) × short diameter $(mm)^2$ × 0.5236 (33). Once tumors reached 50 to 100 mm^3, the mice were surgically castrated under general anesthesia with isoflurane and randomized into two cohorts and then implanted s.c. between the shoulders with 21-day release pellets, either BPA (n = 11; 12.5 mg) or placebo (n = 12; Innovative Research of America, Saratoga, FL). This constituted day 0 of treatment. After 35 days postcastration, mice were euthanized according to University protocol, at which point tumors were harvested, fixed in formalin, and embedded in paraffin for further histochemical analyses.

Serum Assays

Blood samples for determination of serum PSA, testosterone, and BPA levels were obtained weekly by tail vein incisions in mice anesthetized with isoflurane. Serum PSA levels were determined by an ELISA kit with a lower limit sensitivity of 1 ng/mL (BioCheck, Inc., Foster City, CA) according to the manufacturer's protocol. PSA doubling time (PSA-DT) was calculated using the following formula: PSA-DT = time (days) × $\log_e$ (2) / [$\log_e$ (PSA2) − $\log_e$ (PSA1); ref. 34]. Serum testosterone levels were determined using the testosterone ELISA kit (Neogen, Lexington, KY) according to the manufacturer's protocol.

Levels of BPA in serum were determined by high mass accuracy-liquid chromatography/mass spectrometry, wherein a 15 μL serum sample was mixed in a deactivated glass vial with 30 μL of a deuterium-labeled BPA-d_{16} (6.7 ng/mL) internal standard (Sigma-Aldrich, St. Louis, MO) in an aqueous solution of 40% acetonitrile. A full loop (2 μL) was injected onto a Waters (Milford, MA) XBridge 3.5 μm C18 column (100 mm × 2.1 mm i.d.) and eluted under isocratic conditions using 3.7 mN ammonium hydroxide with 40% acetonitrile at 208 μL/min using a Thermo Finnigan (Waltham, MA) Surveyor MS pump coupled with a Micro AS autosampler. Subsequent analysis was done using a Thermo Finnigan LTQ-FT mass spectrometer. Electrospray conditions were as follows: capillary temperature, 325°C; source voltage, 4.5 kV; sheath gas (nitrogen), 30 units; and auxiliary gas (nitrogen), 10 units. Instrument voltages were optimized using tetradecanoate anion (m/z 227.20165) from column bleed. Spectra were acquired in the Fourier transform ion cyclotron resonance portion of the instrument in negative ion profile mode; a broad mass range of m/z 220.11 to m/z 250.11 was required to observe both the deprotonated BPA ion (m/z 227.10775) and its labeled analogue (m/z 241.19563). Resolution was set at 12,500 to provide a rapid duty cycle while still providing ample separation from interferences due to column bleed. The FTMS SIMS AGC Target was set at 500,000 with a maximum ion injection time of 1,500 ms.

BPA standards 1.0, 2.5, 10, 20, 25, 30, 40, 50, 100, and 250 ng/mL were run before and after the serum samples to verify drift and used to calculate serum BPA levels. The limit of detection was 2 ng/mL in serum.

H&E Staining

Paraffin-embedded LNCaP xenograft tumors were sliced into 5-μm sections using a Leica (Bannockburn, IL) microtome (model RM 2125). Tissue sections were deparaffinized by immersion in xylene using 3 × 5 min washes and rehydrated stepwise to 70% ethanol, with a final incubation in deionized water. Slides were stained in Harris' hematoxylin for 30 s, rinsed in water for 4 min, and then stained in Harris eosin for 45 s. Both reagents were purchased from Poly Scientific (Bay Shore, NY). Subsequently, sections were incubated stepwise to 100% ethanol, cleared in xylene using 3 × 5 min washes, and mounted using Permount (Fisher Scientific, FairLawn, NJ).

Immunohistochemistry

Following the deparaffinization and rehydration procedure described above, antigen retrieval was achieved by boiling the slides in a 600 W microwave using an antigen unmasking solution (Vector Laboratories, Inc., Burlingame, CA) for 5 min at full power and then for 20 min at 30% power. Slides were removed from the antigen retrieval solution after 1 h at room temperature and rinsed in PBS, and peroxidase activity was subsequently quenched by 15 min of incubation in H_2O_2 blocking reagent (DAKO, Carpinteria, CA). Tissue sections were processed using a Vectastain Elite avidin-biotin complex method rabbit staining kit according to the manufacturer's specifications (Vector Laboratories). The following primary rabbit polyclonal antibodies, from Santa Cruz Biotechnology (Santa Cruz, CA), were diluted in PBS and incubated overnight at 4°C: 1:12,500 anti-androgen receptor (N-20), 1:1,000 anti-p21 (C-19), and 1:1,000 anti-cyclin D3 (C-16). The antigen was visualized using a 3,3′-diaminobenzidine substrate kit for peroxidase (Vector Laboratories) using 2 min of development. Omission of the primary antibodies yielded no 3,3′-diaminobenzidine reactivity (data not shown). Nuclei were visualized by counterstaining with Harris hematoxylin and further processed as described above.

Bromodeoxyuridine Staining

Sections from LNCaP xenograft tumors that had been labeled *in vivo* with 10 mmol/L bromodeoxyuridine (BrdUrd) for 1 h before sacrifice were deparaffinized, rehydrated, and peroxidase quenched as described above. Antigen retrieval was accomplished by 10 min of incubation in a 37°C humidified chamber using 1:6 dilution of prewarmed trypsin concentrate/trypsin diluent 1B (93-3943, Zymed Laboratories, San Francisco, CA) and rinsed in deionized water. The DNA was denatured with 2 N HCl and rinsed in PBS. Sections were blocked for 30 min at room temperature with 2% normal rabbit serum in an antibody dilution buffer [0.01 mol/L PBS (pH 7.2), 1% bovine serum albumin, 0.1% fish skin gelatin, 0.05% sodium azide] containing 0.1% Triton X-100 and 0.05% Tween 20. Sections were then probed for 1 h in a 37°C humidified chamber using a 1:100 dilution of rat anti-BrdUrd [BU1/75 (ICR1) Accurate Chemical & Scientific, Westbury, NY] in antibody dilution buffer. All remaining steps were conducted at room temperature. Sections were rinsed in PBS and incubated for 30 min using a 1:50 dilution of biotinylated rabbit anti-rat IgG in PBS containing 0.05% sodium azide. Following a PBS wash, BrdUrd was visualized using a 1:200 dilution of horseradish peroxidase-streptavidin in PBS containing 0.05% thimerosal. The biotinylated secondary and streptavidin conjugate were from Vector Laboratories. Antigen development, counterstaining, dehydration, and clearing were done as described above.

Terminal Deoxynucleotidyl Transferase–Mediated dUTP Nick End Labeling Staining

Sections from LNCaP xenograft tumors were deparaffinized and rehydrated as described above and then stained using the DeadEnd Colorimetric terminal deoxynucleotidyl transferase–mediated dUTP nick end labeling (TUNEL) System according to the manufacturer's specifications (Promega, Madison, WI). The immersion of slides into paraformaldehyde was omitted and a 10-min incubation of proteinase K was optimal for permeabilization of the tissue. To generate a positive control, a random tumor section was treated with DNase I (1.0 unit/mL) for 10 min.

Counting and Statistical Assessment

Images were digitally captured (1,315 × 1,033 pixels) using Spot version 4.09 (Diagnostic Instruments, Sterling Heights, MI) on a Nikon (Melville, NY) Microphot-FXA microscope at ×20 or ×40 magnification. Triplicate images from each slide for BrdUrd were counted blind using MetaMorph version 6.3 (Molecular Devices, Sunnyvale, CA), and to ensure accuracy, a digital 7 × 7 grid was applied to each image. Only the center 5 × 5 grid was counted. Statistical analyses for BrdUrd were determined using Student's t test. Statistical analyses for tumor growth and serum PSA were determined used repeated measures one-way ANOVA followed by a Tukey's multiple comparison test. Statistical values of $P < 0.05$ were considered significant. Data are expressed as means ± SE.

Cell Cycle Analyses

Asynchronous LNCaP cells were seeded at 3.5×10^5 per 6-cm dish into appropriate culture conditions, CDT + ethanol (vehicle control), CDT plus 1 μmol/L BPA, CDT plus 1 nmol/L BPA, or 1 μmol/L paclitaxel (apoptotic positive control), and allowed to propagate for either 24 or 72 h. Adherent cells and culture medium were collected via trypsinization and fixed in 80% ice-cold ethanol. To determine percentage of cells with sub-2N DNA content for each culture condition, fixed cells were resuspended in ~1 mL propidium iodide staining solution (50 μg/mL propidium iodide and 40 μg/mL RNase). DNA content was then determined by flow cytometry analysis using a Coulter Epics XL (Beckman Coulter, Miami, FL) with a 488-nm argon-ion laser.

Reverse Transcription-PCR

LNCaP cells (10^6) were seeded onto poly-L-lysine–coated plates and incubated for 48 h in CDT medium as described above. Subsequently, cells were washed with

PBS, and CDT medium with BPA (1 nmol/L) was added for 24 h. Trizol reagent was used to extract total RNA, of which 5 μg were used to generate the cDNA template using the ThermoScript Reverse Transcription-PCR System according to the random hexamer protocol (Invitrogen, Carlsbad, CA). PCRs were done with the following intron spanning primer sets (amplicon sizes are indicated): vascular endothelial growth factor (VEGF; 226 bp), 5′-CTTTCTGCTGTCTTGGGTGCATTG-3′ (forward) and 5′-CACAGGATGGCTTGAAGATGTACTCG-3′ (reverse) and glyceraldehyde-3-phosphate dehydrogenase (597 bp), 5′-CCACCCATGGCAAATTCCATGGCA-3′ (forward) and 5′-TCTAGACGGCAGGTCAGGTCCACC-3′ (reverse). Amplifications were done using Taq DNA polymerase in buffer B (Promega) and conditions for each primer set were as follows: VEGF, 95°C for 5 min; 45 cycles of 95°C for 15 s, 57°C for 15 s, and 70°C for 30 s, with a final extension of 72°C for 5 min. Glyceraldehyde-3-phosphate dehydrogenase, 94°C for 2 min; 27 cycles of 94°C for 30 s, 57°C for 45 s, and 72°C for 50 s, with a final extension of 72°C for 5 min.

Results

Previously, we have shown that nanomolar levels of BPA provide mitogenic stimuli to androgen-dependent prostatic adenocarcinoma cells expressing somatic mutations of the androgen receptor (28, 29). Given the importance of the androgen receptor for prostate cancer growth and progression, it was imperative to examine the effect of BPA on the response to standard therapeutic intervention *in vivo*. For these experiments, the LNCaP xenograft model was used, which expresses an endogenous BPA-responsive androgen receptor mutant (AR-*T877A*; ref. 28) and requires androgen receptor activation for tumor growth (24). After androgen ablation, this xenograft model undergoes a cytostatic response, which persists until recurrent tumors form (35). Therefore, we assessed the influence of BPA on recurrent tumor formation. For these studies, LNCaP cells were injected s.c. into flanks of intact athymic male mice and tumors allowed to form. Once tumors reached a volume approximating 100 mm^3, the mice were surgically castrated and randomized into two cohorts. The first cohort was implanted with 21-day BPA time-release pellets (12.5 mg total BPA) at the time of castration. Concurrently, the second cohort was implanted with placebo pellets.

To validate conditions approximating ADT, serum testosterone levels were measured postcastration, as shown in Fig. 1A. Testosterone levels in age-matched intact male mice were found to be in the range of 1.2 ng/mL, which is within the physiologic range reported previously (36, 37). As expected, testosterone was virtually undetectable (0.003–0.162 ng/mL) in castrated mice regardless of the treatment (placebo or BPA), showing that established LNCaP tumors in both groups were exposed to minimal circulating androgen. Serum BPA levels of mice implanted in parallel with the BPA or placebo pellets were examined over the proposed time course of the experiment (0–35 days postcastration). Mass spectrometry was used as a reliable, sensitive assay to quantify BPA levels in serum, similar to previous reports (38, 39). As shown in Fig. 1B, BPA levels were readily detected as a single peak (Fig. 1B, *inset*), and confidence in quantification was achieved at a lower limit of 2 ng/mL (data not shown). No BPA was detected in the placebo-treated mice (data not shown), whereas mice implanted with the BPA release pellets exhibited a gradual decline in BPA over the time course (Fig. 1B). Average BPA levels were highest at day 7 (27 ng/mL) and undetectable by day 35. The levels of BPA exposure match well with reported doses for human exposure (reviewed in ref. 40). Therefore, the system used models the consequence of environmentally relevant BPA exposure on prostate cancer growth after androgen deprivation.

To assess tumor growth, tumor volumes from each cohort were monitored weekly for the duration of the

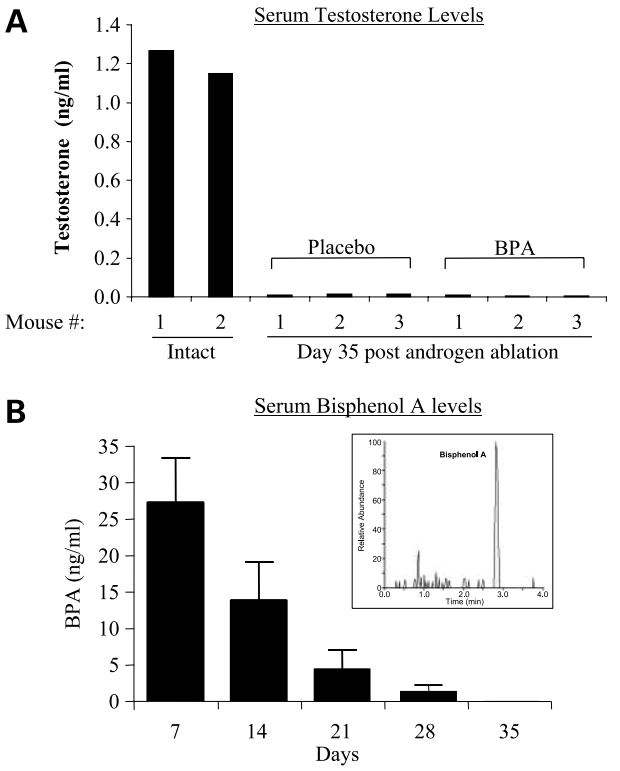

Figure 1. Effects of treatment on serum testosterone and BPA levels. **A,** blood samples were collected from either intact male athymic mice or mice bearing LNCaP prostate tumors treated with either placebo or BPA 21-day time-release pellets (12.5 mg) following 35 d of androgen withdrawal. Testosterone serum concentrations were measured using an enzymatic immunoassay. The data represent individual animal measurements: intact mice, $n = 2$; placebo-treated mice, $n = 3$; and BPA-treated mice, $n = 3$. **B,** parallel studies of mice implanted with either placebo or BPA time-release pellets ($n = 4$ for each group) were used to monitor serum BPA levels over the experimental time course by high mass accuracy-liquid chromatography/mass spectrometry. *Inset,* representative ion chromatogram from day 21 serum taken from a BPA-implanted mouse. No detectable BPA was found in placebo mice (data not shown). *Columns,* average serum BPA levels in mice implanted with BPA time-release pellets; *bars,* SE.

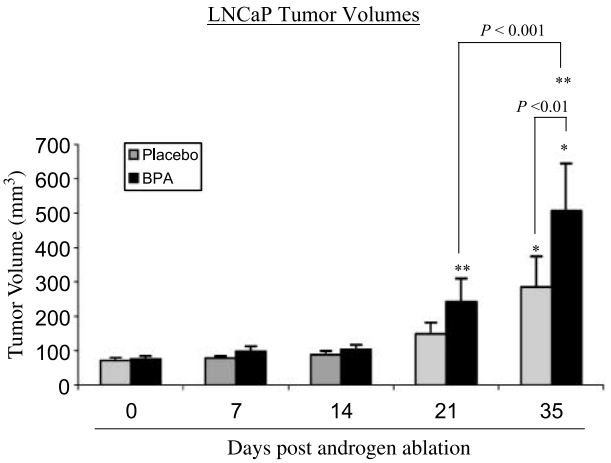

Figure 2. BPA exposure reduces the efficacy of androgen deprivation on tumor growth. Once xenograft tumors achieved the approximate volume of 100 mm^3, mice were surgically castrated, randomly selected, and implanted s.c. with either placebo or BPA 21-d time-release pellets (12.5 mg). Tumor volume was measured weekly and calculated by the formula: volume (mm^3) = long diameter (mm) × short diameter $(mm)^2$ × 0.5236. *Columns,* average tumor size among the groups (n = 12 animals in the placebo-treated group; n = 11 animals for BPA-treated group); *bars,* SE. *, $P < 0.01$; **, $P < 0.001$.

experiment. As shown in Fig. 2, LNCaP tumor volumes remained relatively static throughout 14 to 21 days postcastration, in agreement with previously published observations (33, 37). Following this time point, tumor growth resumed and steadily increased in the placebo group, reflecting the progression to therapeutic resistance reported for this model system under conditions of androgen withdrawal. In the BPA-treated cohort, tumor growth was also apparent by 21 days. This enhanced tumor growth trend continued through day 35 and resulted in significantly larger tumors (284 ± 89 and 507 ± 137.5 mm^3 for placebo- and BPA-treated groups, respectively; $P < 0.01$). Thus, these data suggest that at relatively low levels, BPA is capable of promoting growth of prostate tumors *in vivo* in the absence of testicular androgen, suggesting that BPA may adversely affect the magnitude of the response to ADT.

To determine if the increase in tumor size was attributed to differences in histologic architecture, analysis of tumor microanatomy was done, as shown in Fig. 3. As evident, all tumors exhibited highly disorganized and multicapsulated architecture with extensive hemorrhage throughout, regardless of the treatment (Fig. 3A, *top, H&E*; data not shown). Additionally, there was little difference in cell size and number, and both cohorts displayed densely packed cells with evident mitotic figures and areas of necrosis (Fig. 3A; data not shown). Androgen receptor expression was subsequently examined, as it has been shown that recurrent (ADT resistant) tumors frequently show more intense androgen receptor immunostaining than the primary lesion, and amplification and/or overexpression are causative for therapeutic relapse (41–46). Androgen receptor was expressed in tumors from both treatment groups, and no discernable differences in androgen receptor levels were observed (Fig. 3A; data not shown). Thus, alterations in androgen receptor expression are unlikely to underlie observed changes in tumor volume. It has been reported that BPA can induce VEGF mRNA expression in the uterus, vagina, and pituitary of Sprague-Dawley rats (47). Thus, we examined VEGF mRNA levels after BPA exposure

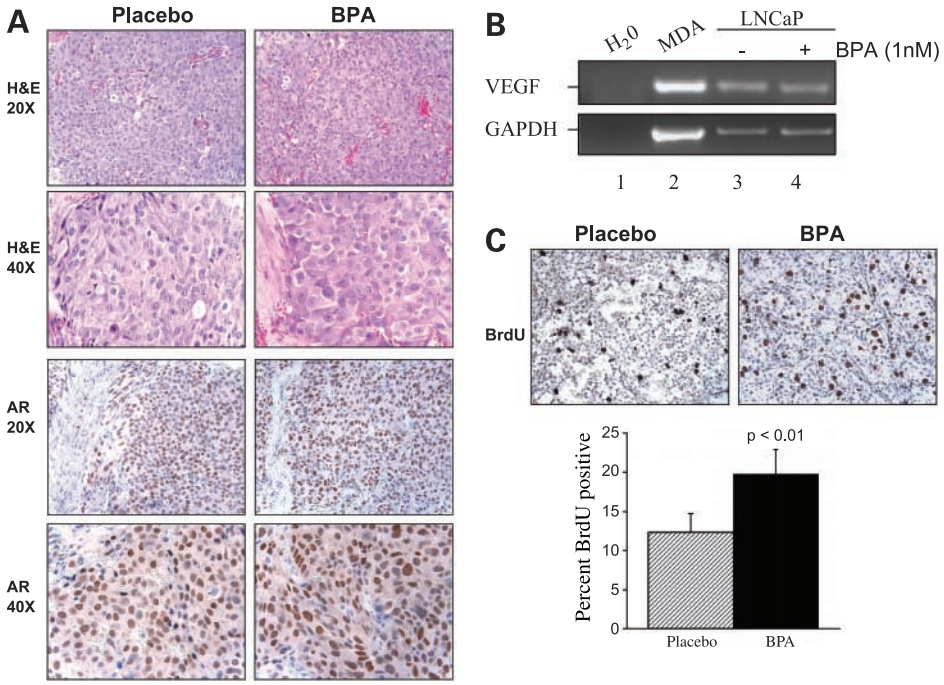

Figure 3. LNCaP tumors treated by ADT in the presence of BPA exhibit increased proliferation. **A,** *top* and *middle top,* general LNCaP prostate tumor architecture in both treatment groups, H&E staining (magnifications, ×20 and ×40); *bottom* and *middle bottom,* immunohistochemical detection of androgen receptor expression (magnifications, ×20 and ×40). **B,** VEGF reverse transcription-PCR on mRNA from MDA-MB-468 (positive control; *lane 2*) or LNCaP cells ±1 nmol/L BPA (*lanes 3* and *4*). Glyceraldehyde-3-phosphate dehydrogenase (*GAPDH*) mRNA was used to control for concentration of RNA in each reaction. **C,** BrdUrd incorporation (*top*; magnification, ×20) and graphical representation (*bottom*) of BrdUrd-positive cells from placebo- or BPA-exposed mice.

in LNCaP cells (Fig. 3B). In this model system, VEGF expression was present but similar in both BPA-treated or control-stimulated cells (Fig. 3B, compare *lanes 3* and *4*), as may be predicted based on pathologic inspection of the tumors. Breast cancer MDA-MB-468 cells were used as a positive control (Fig. 3B, *lane 2*; ref. 48), and glyceraldehyde-3-phosphate dehydrogenase served as the internal control for mRNA concentration (Fig. 3B, *bottom*). Combined, these data indicate that the histopathologic features of the LNCaP xenografts are not significantly altered by BPA exposure.

To determine if the differences in tumor size were attributed to enhanced proliferation, animals from both cohorts were injected with BrdUrd before sacrifice, and tumors were analyzed for BrdUrd incorporation by immunohistochemistry (Fig. 3C). BrdUrd labeling revealed that the BPA-treated tumors exhibited increased proliferative indices compared with the placebo-treated cohort (20% compared with 12%, respectively; $P < 0.01$; Fig. 3C, *bottom*). These findings show that tumors exposed to BPA have a higher proportion of cells actively engaged in the cell cycle, thus contributing to the increased Volume and enhanced growth rate of BPA-exposed tumors. Together, these data strongly implicate BPA as a mitogenic stimulus for prostate tumors harboring the AR-*T877A* mutation.

Increased tumor size in the BPA-treated animals could be attributed to mechanisms other than enhanced cellular proliferation, such as a reduction in apoptotic rates. To test this, cells were initially examined for sub-2N DNA content, an indication of apoptotic DNA fragmentation and degradation. BPA failed to induce quantifiable changes in apoptosis in LNCaP cells in culture at any BPA dose tested (1 μmol/L–1 nmol/L) following either 24 or 72 h of exposure (Fig. 4A, *middle*). Conversely, the chemotherapeutic agent paclitaxel induced accumulation of marked sub-2N DNA content and provided a positive control (Fig. 4A, *bottom*). The apoptotic index was also monitored *in vivo* through standard TUNEL assays in the recovered xenograft tumors. As shown in Fig. 4B, no perceptible distinctions in apoptotic cells between the BPA and placebo groups were apparent (Fig. 4B, *middle* and *left*, respectively). Overall, apoptotic rates were low in both cohorts, although the positive control (DNase treated) tumors showed high levels of positivity (Fig. 4B, *right*). Together, these data indicate that BPA exposure is unlikely to alter rates of cell death in prostate cancer cells.

In patients, tumor burden is typically monitored using a serum biomarker, PSA, which is a well-defined androgen receptor target gene (34). PSA detection is a powerful measure of tumor size/growth and progression to hormone therapy-resistant prostate cancer and is invariably associated with rapidly rising PSA levels, termed biochemical recurrence or failure (49). Previous studies have shown that BPA can activate AR-*T877A* to induce PSA expression (28, 29). Thus, these data indicate that BPA may affect the timing of biochemical recurrence that precedes visible tumor formation. PSA expression is human specific; therefore, to validate our studies, we measured serum PSA in both cohorts (Fig. 5A). In the control (placebo treated) group, PSA levels dropped 75% postcastration, in accordance with the published literature (Fig. 5A, compare *striped columns*; days 0 and 7; refs. 32, 33). By day 21 in the placebo cohort, PSA levels rose to 40 ng/mL and remained static at this position through the remainder of the testing period. In the BPA-treated group, the nadir PSA levels after androgen deprivation were higher compared with the placebo-treated group (day 7), and elevated PSA levels in the BPA group continued until the end point of the experiment, wherein PSA levels were increased 50% ($P < 0.01$). Moreover, the increase in PSA in the BPA-exposed group from days 21 to 35 was significant ($P < 0.01$), whereas the placebo-treated group did not yield a statistically significant increase in PSA.

The rate at which PSA levels rose also increased in the BPA cohort compared with placebo-treated animals (Fig. 5B). PSA doubling time (PSA-DT) is often used clinically to monitor ADT relapse or biochemical failure (34, 50, 51). In Fig. 5B, serum PSA levels were plotted as relative change over the nadir and the following formula was used to determine the average doubling time for PSA: PSA-DT = time (days) $\times \log_e (2) / [\log_e (PSA2) - \log_e (PSA1)$; ref. 34]. BPA-treated tumors secreted PSA at a dramatically elevated rate (PSA-DT, 0.68 days) compared with placebo-treated tumors (PSA-DT, 1.4 days). As this measurement is correlated with ADT resistance and tumor recurrence (50), these data show that environmentally relevant levels of circulating BPA could exacerbate progression from androgen-sensitive disease state to androgen-independent, therapy-resistant cancer in prostate tumors harboring the AR-*T877A* mutation.

Discussion

This study shows that environmentally relevant levels of exposure to a prevalent endocrine-disrupting compound, BPA, could promote prostate cancer growth and advance biochemical recurrence in tumors harboring the endogenous AR-*T877A* mutation. Thus, these results suggest that incidental exposure to BPA may facilitate the transition of a subset of prostate tumors to ADT resistance and therefore may influence the duration and magnitude of the therapeutic response in prostate cancer patients.

Endocrine-disrupting compounds have pleiotropic influences on prostate cancer risk, development, and progression (reviewed in ref. 52). The various effects include initiating changes in prostatic development, acting as potential mutagens, or directly modulating the androgen receptor pathway. Previous studies of BPA action in prostate cancer cell lines revealed that the effect of BPA on androgen-independent proliferation is likely confined to tumors expressing certain somatic androgen receptor mutations (29). ADT is known to select for mutations of the androgen receptor, most commonly in the ligand-binding domain (53). These somatic mutations change the conformation of this domain, thereby facilitating activation

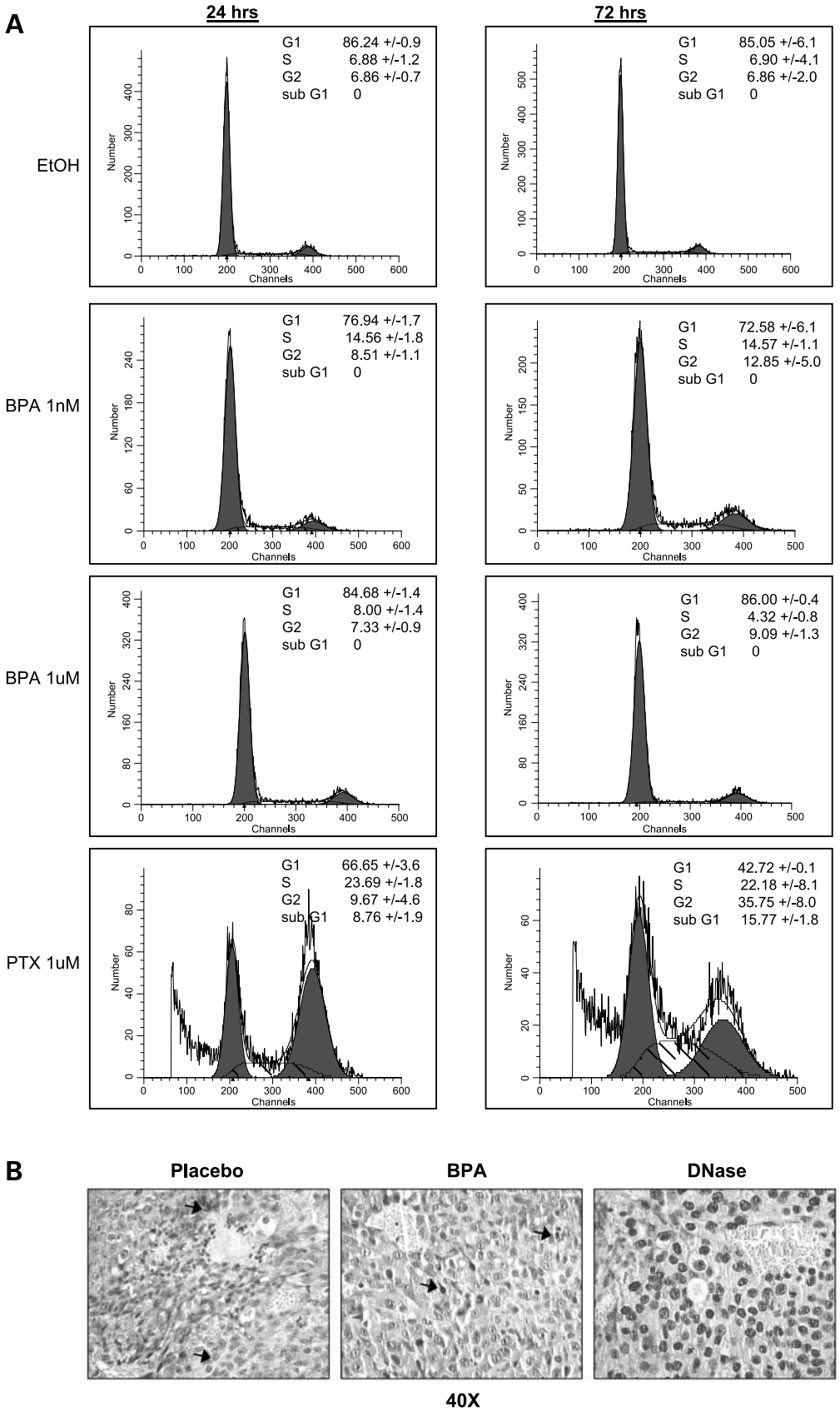

Figure 4. Apoptotic rates are indistinguishable in placebo- or BPA-treated cohorts. **A,** LNCaP cells treated with either ethanol (*EtOH*; vehicle control; *top*), 1 nmol/L or 1 μmol/L BPA (*middle*), or 1 μmol/L paclitaxel (*PTX*; positive apoptotic control) for indicated time points were analyzed for sub-2N DNA content by propidium iodide staining and fluorescence-activated cell sorting analyses. Quantification of cell cycle profile. **B,** representative TUNEL images from xenograft tumor sections from placebo-exposed (*left*) or BPA-exposed (*middle*) mice (*arrows*, positive nuclei). DNase-treated section included as a positive control (*right*). Magnification, ×40.

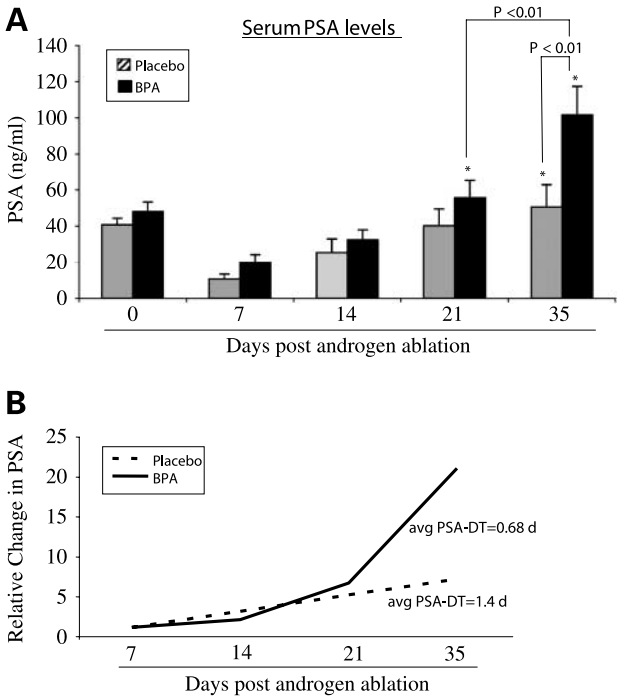

Figure 5. BPA exposure advances progression to therapy resistance. Blood samples were collected weekly starting at day 0 of the experiment, which corresponded to surgical castration. Serum PSA levels were determined by enzymatic immunoassay. **A**, tumor-derived serum PSA concentration. After initial decrease in PSA levels (day 7 postcastration versus day 0), PSA concentrations started to increase again at day 21 of androgen ablation, reaching statistical significance between placebo- and BPA-treated groups at day 35. *, $P < 0.01$. $n = 12$ in the placebo-treated group and $n = 11$ in BPA-treated group. Results were average concentration. *Columns,* PSA (ng/mL); *bars,* SE. **B**, rate of PSA increase for both placebo-and BPA-exposed animals. Change in PSA was plotted relative to the nadir for each cohort. PSA-DT was calculated as PSA-DT = time (days) $\times \log_e (2) / [\log_e (PSA2) - \log_e (PSA1)]$; ref. 34].

by noncanonical endogenous steroid hormones (e.g., estrogen, cortisol, and progesterone; refs. 27, 54) as well as converting therapeutic androgen receptor antagonists into agonists (e.g., flutamide; refs. 27, 55–57). Several tumor-derived androgen receptor mutants are responsive to BPA, including AR-*T877A*, AR-*H874Y*, AR-*V715M*, and AR-*T877S* (29). AR-*T877A*, the most frequently reported somatic mutation in prostate cancer, is suggested to arise in 8% to 31% of therapy-resistant tumors (27, 58). The present study addresses the influence of BPA in the presence of this prevalent androgen receptor mutant protein. Currently, the influence of BPA on prostate cancer therapeutic response in the presence of the remaining androgen receptor mutants is hindered by the paucity of appropriate model systems. Thus, further investigation is needed to determine whether the effect of BPA on androgen deprivation is limited to tumors expressing the AR-*T877A* mutant.

The ability of BPA to impinge on the AR-*T877A* mutant is proposed to underlie its proliferative effect on tumor growth *in vivo*. Mouse tumors exposed to BPA levels relevant to human exposure (between 2 and 27 ng/mL; Fig. 1B; ref. 40) for 35 days after surgical castration showed an increased tumor size relative to the placebo-treated group (Fig. 2). Vascular density in prostate tumors directly correlates with advanced tumor stage and metastatic development (59, 60). Given that angiogenesis can be promoted by estrogen (61) and that BPA is a known estrogen mimic, histoarchitectural features were evaluated between the groups to address the possibility that altered tumor size was attributed to unbalanced vascular density. No distinctions were observed between the two groups, and no variances in VEGF production were detected following BPA exposure (Fig. 3), indicating that the disparity in size was likely attributed to enhanced proliferation. This hypothesis was supported by analyses of proliferative index, wherein BPA-exposed tumors showed a higher overall BrdUrd incorporation rate (Fig. 3C). Thus, the data shown indicate that BPA mediates increased cellular proliferation, most likely through AR-*T877A*. This prediction is strongly supported by *in vitro* analyses of BPA effects on AR-T877A (28, 29) and in the observation that elevated PSA levels in the BPA-treated cohort preceded significant induction of tumor size (Figs. 2 and 5).

It has been shown previously that BPA can alter expression of several key cell cycle regulators, including p21, cyclin A, and the D type cyclins (29). Although preliminary immunohistochemical investigations revealed some alteration in p21 expression as a function of BPA exposure (data not shown), these trends did not reach statistical significance. AKT activity was also monitored, and BPA exposure failed to alter the levels of AKT phosphorylation in this model system (data not shown). However, it should be noted that LNCaP cells harbor constitutively active AKT (62, 63) that is not further activated by androgen receptor ligands (including dihydrotestosterone; ref. 64). Additionally, a recent study by Ho et al. (65) found that mice exposed to low-level BPA during development exhibited alternations in DNA methylation patterns in cell signaling genes, contributing to increased incidence of precancerous lesions within the mouse prostate. These data indicate that altered methylation of genes associated with proliferation may, in part, underlie the response to BPA. Therefore, the precise mechanisms by which BPA influences cell cycle progression *in vivo* will be the subject of future analyses.

The transition to therapeutic resistance in prostate cancer is frequently associated with enhanced androgen receptor expression (43, 44, 46, 66). Increased androgen receptor is both necessary and sufficient to render prostate cancer cells resistant to anti-androgen therapy, as amplified androgen receptor enhances the basal level response to low residual hormone as well as modifies the androgen receptor response to antagonists (42). Exposure to low levels of estrogenic compounds, including BPA, during neonatal development alters androgen receptor signaling and results in changes in prostate development and size (67). Moreover, it is notable that BPA has been shown to alter

androgen receptor levels *in vivo* (68). Therefore, we analyzed androgen receptor expression in the xenograft tumors and observed no differences in androgen receptor levels between BPA- and placebo-exposed tumors (Fig. 3A; data not shown). Therefore, the transition to therapeutic resistance and PSA elevation was likely associated with AR-*T877A* activation, rather than elevation of androgen receptor protein levels.

The observation that BPA-exposed tumors exhibited increased PSA secretion is consistent with previous reports *in vitro*, wherein BPA induced PSA mRNA expression in LNCaP cells (28, 29). This finding is of importance, as progression to therapy-resistant prostate cancer is often associated clinically with rapidly rising PSA levels (49). Given the relationship between androgen receptor activity and prostate cancer proliferation, PSA serum levels are used clinically to diagnose prostate cancer and monitor tumor progression (16). Moreover, in both tissue culture and xenograft model systems of prostate cancer, a reduction in PSA follows inactivation of androgen receptor (either through direct androgen receptor antagonists or androgen deprivation treatment) and a recurrence of PSA expression is seen after supplementation with androgen or androgen receptor agonists and is concomitant with the onset of ADT resistance. Throughout the duration of this study period, serum PSA levels were monitored and BPA-exposed tumors elicited an earlier and more dramatic elevation in PSA compared with the placebo-treated animals. PSA-DT was significantly enhanced in the BPA-treated group versus the placebo control group. PSA-DT is used clinically to monitor ADT relapse, and rapidly rising PSA after intervention is referred to as biochemical failure (34, 50, 51). Thus, the examined xenograft model system exhibited a shorter time to biochemical recurrence after BPA exposure (Fig. 5). Although these studies implicate BPA as a contributing factor for therapy resistance in tumors challenged by ADT [particularly with gonaclotropin-releasing hormone (GnRH) agonists or finasteride] and expressing BPA-sensitive androgen receptor mutants, it is imperative to note that direct androgen receptor antagonists, such as bicalutamide, effectively counter BPA activity in cultured cells (28, 29) Thus, any increase in PSA that is attributed to BPA exposure would be expected to be reversed through the administration of such androgen receptor antagonists. Additional studies to address the long-term effect of BPA exposure on the response to androgen receptor antagonists are currently under way.

In summary, this study suggests that exposure of advanced prostate tumors expressing somatic mutations in the androgen receptor gene (that frequently occur in ADT; refs. 18, 19, 21) to a highly prevalent endocrine-disrupting compound can facilitate ADT bypass and advance tumor recurrence. Hence, our study lays a foundation for defining the clinical variables wherein BPA and other endocrine-disrupting chemicals may contribute to prostate cancer progression and alter treatment success.

Acknowledgments

We thank Dr. Monica P. Revelo (UC Department of Pathology) for pathologic assessment; Dr. Eric R. Hugo (UC Department of Cell and Cancer Biology) for providing the VEGF primers and MDA-MB-468 cDNA; Drs. Erik Knudsen, Craig Burd, and Lisa Morey as well as Nick Olshavsky, Kevin Link, William Zagorski, and Ankur Sharma (UC Department of Cell and Cancer Biology) for insightful commentary and assistance with editing of the manuscript.

References

1. Jemal A, Murray T, Ward E, et al. Cancer statistics, 2005. CA Cancer J Clin 2005;55:10 – 30.

2. Sharifi N, Farrar WL. Androgen receptor as a therapeutic target for androgen independent prostate cancer. Am J Ther 2006;13:166 – 70.

3. Damber JE, Khatami A. Surgical treatment of localized prostate cancer. Acta Oncol 2005;44:599 – 604.

4. Kirkpatrick JP, Anscher MS. Radiotherapy for locally recurrent prostate cancer. Clin Adv Hematol Oncol 2005;3:933 – 42.

5. Zeliadt SB, Ramsey SD, Penson DF, et al. Why do men choose one treatment over another? A review of patient decision making for localized prostate cancer. Cancer 2006;106:1865 – 74.

6. Dehm SM, Tindall DJ. Molecular regulation of androgen action in prostate cancer. J Cell Biochem 2006;99:333 – 44.

7. Eder IE, Haag P, Bartsch G, Klocker H. Targeting the androgen receptor in hormone-refractory prostate cancer-new concepts. Future Oncol 2005; 1:93 – 101.

8. Denmeade SR, Isaacs JT. A history of prostate cancer treatment. Nat Rev Cancer 2002;2:389 – 96.

9. Denis LJ. The role of active treatment in early prostate cancer. Radiother Oncol 2000;57:251 – 8.

10. Dyrstad SW, Shah P, Rao K. Chemotherapy for prostate cancer. Curr Pharm Des 2006;12:819 – 37.

11. Trapman J, Brinkmann AO. The androgen receptor in prostate cancer. Pathol Res Pract 1996;192:752 – 60.

12. Shang Y, Myers M, Brown M. Formation of the androgen receptor transcription complex. Mol Cell 2002;9:601 – 10.

13. Mendelsohn LG. Prostate cancer and the androgen receptor: strategies for the development of novel therapeutics. Prog Drug Res 2000;55:213 – 33.

14. Hirawat S, Budman DR, Kreis W. The androgen receptor: structure, mutations, and antiandrogens. Cancer Invest 2003;21:400 – 17.

15. Freeman SN, Mainwaring WI, Furr BJ. A possible explanation for the peripheral selectivity of a novel non-steroidal pure antiandrogen, Casodex (ICI 176,334). Br J Cancer 1989;60:664 – 8.

16. Stephan C, Jung K, Diamandis EP, Rittenhouse HG, Lein M, Loening SA. Prostate-specific antigen, its molecular forms, and other kallikrein markers for detection of prostate cancer. Urology 2002;59:2 – 8.

17. Feldman BJ, Feldman D. The development of androgen-independent prostate cancer. Nat Rev Cancer 2001;1:34 – 45.

18. Taplin ME, Bubley GJ, Shuster TD, et al. Mutation of the androgen-receptor gene in metastatic androgen-independent prostate cancer. N Engl J Med 1995;332:1393 – 8.

19. Taplin ME, Bubley GJ, Ko YJ, et al. Selection for androgen receptor mutations in prostate cancers treated with androgen antagonist. Cancer Res 1999;59:2511 – 5.

20. Taplin ME, Rajeshkumar B, Halabi S, et al. Androgen receptor mutations in androgen-independent prostate cancer: Cancer and Leukemia Group B Study 9663. J Clin Oncol 2003;21:2673 – 8.

21. Taplin ME, Balk SP. Androgen receptor: a key molecule in the progression of prostate cancer to hormone independence. J Cell Biochem 2004;91:483 – 90.

22. Tilley WD, Buchanan G, Hickey TE, Bentel JM. Mutations in the androgen receptor gene are associated with progression of human prostate cancer to androgen independence. Clin Cancer Res 1996;2:277 – 85.

23. Zhao XY, Malloy PJ, Krishnan AV, et al. Glucocorticoids can promote androgen-independent growth of prostate cancer cells through a mutated androgen receptor. Nat Med 2000;6:703 – 6.

24. Veldscholte J, Berrevoets CA, Brinkmann AO, Grootegoed JA, Mulder E. Anti-androgens and the mutated androgen receptor of LNCaP cells:

differential effects on binding affinity, heat-shock protein interaction, and transcription activation. Biochemistry 1992;31:2393 – 9.

25. Veldscholte J, Berrevoets CA, Ris-Stalpers C, et al. The androgen receptor in LNCaP cells contains a mutation in the ligand binding domain which affects steroid binding characteristics and response to antiandrogens. J Steroid Biochem Mol Biol 1992;41:665 – 9.

26. Veldscholte J, Ris-Stalpers C, Kuiper GG, et al. A mutation in the ligand binding domain of the androgen receptor of human LNCaP cells affects steroid binding characteristics and response to anti-androgens. Biochem Biophys Res Commun 1990;173:534 – 40.

27. Suzuki H, Sato N, Watabe Y, Masai M, Seino S, Shimazaki J. Androgen receptor gene mutations in human prostate cancer. J Steroid Biochem Mol Biol 1993;46:759 – 65.

28. Wetherill YB, Petre CE, Monk KR, Puga A, Knudsen KE. The xenoestrogen bisphenol A induces inappropriate androgen receptor activation and mitogenesis in prostatic adenocarcinoma cells. Mol Cancer Ther 2002;1:515 – 24.

29. Wetherill YB, Fisher NL, Staubach A, Danielsen M, de Vere White RW, Knudsen KE. Xenoestrogen action in prostate cancer: pleiotropic effects dependent on androgen receptor status. Cancer Res 2005;65:54 – 65.

30. Haighton LA, Hlywka JJ, Doull J, Kroes R, Lynch BS, Munro IC. An evaluation of the possible carcinogenicity of bisphenol A to humans. Regul Toxicol Pharmacol 2002;35:238 – 54.

31. Calafat AM, Kuklenyik Z, Reidy JA, Caudill SP, Ekong J, Needham LL. Urinary concentrations of bisphenol A and 4-nonylphenol in a human reference population. Environ Health Perspect 2005;113:391 – 5.

32. Sato N, Gleave ME, Bruchovsky N, Rennie PS, Beraldi E, Sullivan LD. A metastatic and androgen-sensitive human prostate cancer model using intraprostatic inoculation of LNCaP cells in SCID mice. Cancer Res 1997; 57:1584 – 9.

33. Gleave M, Hsieh JT, Gao CA, von Eschenbach AC, Chung LW. Acceleration of human prostate cancer growth *in vivo* by factors produced by prostate and bone fibroblasts. Cancer Res 1991;51:3753 – 61.

34. Haukaas SA, Halvorsen OJ, Daehlin L, Hostmark J, Akslen LA. Is preoperative serum prostate-specific antigen level significantly related to clinical recurrence after radical retropubic prostatectomy for localized prostate cancer? BJU Int 2006;97:51 – 5.

35. Lim DJ, Liu XL, Sutkowski DM, Braun EJ, Lee C, Kozlowski JM. Growth of an androgen-sensitive human prostate cancer cell line, LNCaP, in nude mice. Prostate 1993;22:109 – 18.

36. Wang J, Eltoum IE, Lamartiniere CA. Genistein alters growth factor signaling in transgenic prostate model (TRAMP). Mol Cell Endocrinol 2004;219:171 – 80.

37. Jin RJ, Wang Y, Masumori N, et al. NE-10 neuroendocrine cancer promotes the LNCaP xenograft growth in castrated mice. Cancer Res 2004;64:5489 – 95.

38. Sajiki J, Takahashi K, Yonekubo J. Sensitive method for the determination of bisphenol-A in serum using two systems of high-performance liquid chromatography. J Chromatogr B Biomed Sci Appl 1999;736:255 – 61.

39. Sambe H, Hoshina K, Hosoya K, Haginaka J. Direct injection analysis of bisphenol A in serum by combination of isotope imprinting with liquid chromatography-mass spectrometry. Analyst 2005;130:38 – 40.

40. Welshons WV, Nagel SC, vom Saal FS. Large effects from small exposures. III. Endocrine mechanisms mediating effects of bisphenol A at levels of human exposure. Endocrinology 2006;147:S56 – 69.

41. Culig Z, Hoffmann J, Erdel M, et al. Switch from antagonist to agonist of the androgen receptor bicalutamide is associated with prostate tumour progression in a new model system. Br J Cancer 1999;81:242 – 51.

42. Chen CD, Welsbie DS, Tran C, et al. Molecular determinants of resistance to antiandrogen therapy. Nat Med 2004;10:33 – 9.

43. Visakorpi T, Hyytinen E, Koivisto P, et al. *In vivo* amplification of the androgen receptor gene and progression of human prostate cancer. Nat Genet 1995;9:401 – 6.

44. Koivisto P, Kononen J, Palmberg C, et al. Androgen receptor gene amplification: a possible molecular mechanism for androgen deprivation therapy failure in prostate cancer. Cancer Res 1997;57:314 – 9.

45. Gregory CW, He B, Johnson RT, et al. A mechanism for androgen receptor-mediated prostate cancer recurrence after androgen deprivation therapy. Cancer Res 2001;61:4315 – 9.

46. Culig Z, Steiner H, Bartsch G, Hobisch A. Mechanisms of endocrine therapy-responsive and -unresponsive prostate tumours. Endocr Relat Cancer 2005;12:229 – 44.

47. Long X, Burke KA, Bigsby RM, Nephew KP. Effects of the xenoestrogen bisphenol A on expression of vascular endothelial growth factor (VEGF) in the rat. Exp Biol Med (Maywood) 2001;226:477 – 83.

48. Weigand M, Hantel P, Kreienberg R, Waltenberger J. Autocrine vascular endothelial growth factor signalling in breast cancer. Evidence from cell lines and primary breast cancer cultures *in vitro*. Angiogenesis 2005;8:197 – 204.

49. Balk SP, Ko YJ, Bubley GJ. Biology of prostate-specific antigen. J Clin Oncol 2003;21:383 – 91.

50. Buyyounouski MK, Hanlon AL, Eisenberg DF, et al. Defining biochemical failure after radiotherapy with and without androgen deprivation for prostate cancer. Int J Radiat Oncol Biol Phys 2005;63:1455 – 62.

51. Pickles T. Prostate-specific antigen (PSA) bounce and other fluctuations: which biochemical relapse definition is least prone to PSA false calls? An analysis of 2030 men treated for prostate cancer with external beam or brachytherapy with or without adjuvant androgen deprivation therapy. Int J Radiat Oncol Biol Phys 2006;64:1355 – 9.

52. Hess-Wilson JK, Knudsen KE. Endocrine disrupting compounds and prostate cancer. Cancer Lett 2006;241:1 – 12.

53. Gottlieb B, Beitel LK, Wu JH, Trifiro M. The androgen receptor gene mutations database (ARDB): 2004 update. Hum Mutat 2004;23:527 – 33.

54. Culig Z, Hobisch A, Cronauer MV, et al. Mutant androgen receptor detected in an advanced-stage prostatic carcinoma is activated by adrenal androgens and progesterone. Mol Endocrinol 1993;7:1541 – 50.

55. Hara T, Miyazaki J, Araki H, et al. Novel mutations of androgen receptor: a possible mechanism of bicalutamide withdrawal syndrome. Cancer Res 2003;63:149 – 53.

56. Chatterjee B. The role of the androgen receptor in the development of prostatic hyperplasia and prostate cancer. Mol Cell Biochem 2003;253: 89 – 101.

57. Bohl CE, Gao W, Miller DD, Bell CE, Dalton JT. Structural basis for antagonism and resistance of bicalutamide in prostate cancer. Proc Natl Acad Sci U S A 2005;102:6201 – 6.

58. Marcelli M, Ittmann M, Mariani S, et al. Androgen receptor mutations in prostate cancer. Cancer Res 2000;60:944 – 9.

59. Weidner N, Carroll PR, Flax J, Blumenfeld W, Folkman J. Tumor angiogenesis correlates with metastasis in invasive prostate carcinoma. Am J Pathol 1993;143:401 – 9.

60. Bigler SA, Deering RE, Brawer MK. Comparison of microscopic vascularity in benign and malignant prostate tissue. Hum Pathol 1993;24: 220 – 6.

61. Seo KH, Lee HS, Jung B, et al. Estrogen enhances angiogenesis through a pathway involving platelet-activating factor-mediated nuclear factor-κB activation. Cancer Res 2004;64:6482 – 8.

62. Chen X, Thakkar H, Tyan F, et al. Constitutively active Akt is an important regulator of TRAIL sensitivity in prostate cancer. Oncogene 2001;20:6073 – 83.

63. Nesterov A, Lu X, Johnson M, Miller GJ, Ivashchenko Y, Kraft AS. Elevated AKT activity protects the prostate cancer cell line LNCaP from TRAIL-induced apoptosis. J Biol Chem 2001;276:10767 – 74.

64. Xu Y, Chen SY, Ross KN, Balk SP. Androgens induce prostate cancer cell proliferation through mammalian target of rapamycin activation and post-transcriptional increases in cyclin D proteins. Cancer Res 2006;66: 7783 – 92.

65. Ho SM, Tang WY, Belmonte de Frausto J, Prins GS. Developmental exposure to estradiol and bisphenol A increases susceptibility to prostate carcinogenesis and epigenetically regulates phosphodiesterase type 4 variant 4. Cancer Res 2006;66:5624 – 32.

66. Zhang H, Yi X, Sun X, et al. Differential gene regulation by the SRC family of coactivators. Genes Dev 2004;18:1753 – 65.

67. Gupta C. Reproductive malformation of the male offspring following maternal exposure to estrogenic chemicals. Proc Soc Exp Biol Med 2000; 224:61 – 8.

68. Ramos JG, Varayoud J, Sonnenschein C, Soto AM, Munoz De Toro M, Luque EH. Prenatal exposure to low doses of bisphenol A alters the periductal stroma and glandular cell function in the rat ventral prostate. Biol Reprod 2001;65:1271 – 7.

Molecular Cancer Therapeutics

Bisphenol A facilitates bypass of androgen ablation therapy in prostate cancer

Yelena B. Wetherill, Janet K. Hess-Wilson, Clay E.S. Comstock, et al.

Mol Cancer Ther 2006;5:3181-3190.